Numerical Simulation of Deposit Shape Evolution During the Spray-Rolling Process

FENGXIAN LI, YUNZHONG LIU, and XIA LUO

The sprayed deposit shape before feeding into the two roller wheels during the spray-rolling process was investigated using mathematical models, tracing the coordinates of a growing deposit with respect to time. Because two deposition surfaces are arranged closely next to each other as in the case of spraying onto two wheels, some important realistic scenarios, such as droplet rebounding and redeposition, and the geometrical features of deposition surface, were considered. Then, the calculated results of the shape evolution were utilized to predict the corresponding drag-in angle, deposit thickness, and the production rate. The calculated values agree well with the experimental data. The results show that the deposit shape and production rate are sensitive to processing parameters such as the roll gap, the roller diameter and rotational speed, the spray distance, and the mass flux distribution in the spray cone. The optimum spray-rolling processing parameters were determined and presented by using an orthogonal design method.

DOI: 10.1007/s11661-012-1274-6

I. INTRODUCTION

SPRAY rolling is a novel metallic semisolid near-net-shape forming technique. It was proposed by E.J. Lavernia and K.M. McHugh in 2003 and may be traced back to A.R.E. Singer's pioneering work in the 1970s.[1,2] Spray rolling combines the advantages of twin-roll casing and spray forming in a single operation and shows promise for providing a new method of plate and strip production resulting in energy and materials saving, a short production run, and high-performance process for the metal industry.[3–5] In spray rolling (Figure 1), the molten aluminum alloy metal stream is atomized into disintegrated, microsized droplets by an inert gas and deposited on the roller surface. Then, the deposited material is dragged into the roll gap and consolidated to a fully dense strip. The spray-rolling process has been under development in few industrial countries.[6–8]

By controlling the process properly, especially the deposit shape and thickness, it is possible to control spray rolling yield in the manufacture of near-net-shape preforms of strips such as 7050 aluminum alloy. An inspection of the available literature demonstrates that the shape models have been developed and applied to describe the deposit shape evolution during spray forming process by dealing with a continuous droplet mass flux or individual droplets.[9–12] Moreover, it is evident that the droplet splashing, redeposition of materials, and topological features of deposition surface are important factors in governing the deposit shape.[13,14] However, it should be noted that the previous work on spray forming focused on deposits only in the shape of a billet, tube, or ring.[15] In spray rolling, two deposition surfaces are arranged closely next to each other. The rebounding of droplets from the surface of one wheel to another, namely the droplet rebounding and redeposition phenomenon, an important factor in governing the deposit shape, should be considered. The dynamics of the spray-rolling process presents a significant challenge for the development of meaningful models. Lin *et al.*[4,5] studied the transient to steady-state transition and the selection of the spray deposition rate during the spray-rolling process. However, little information has been obtained for the deposit shape evolution.

This article provides a theoretical analysis of deposit shape evolution during spray rolling by considering the geometrical features of deposition surface and the droplet rebounding and redeposition phenomenon. We focus on determining the entry angle for spray-rolling process in order to obtain a continuous operation. The simulation results can be compared with the experimental results via deposit thickness and strip production rate.

II. MODELING

A. *Mass Flux Distribution in the Spray Cone*

In the linear atomizer nozzle, the slit for the molten metal delivery is parallel to the roll axes. A cross-sectional geometry normal to the roll axes is used to represent the overall geometry of the spray-rolled material, as shown in Figure 2(a). In order to deal with the complicated geometrical features of deposition surface, a function of the spray following a Gaussian distribution was used.[15]

FENGXIAN LI and XIA LUO, Ph.D. Candidates, and YUN ZHONG LIU, Professor, are with the National Engineering Research Center of Near-Net-Shape Forming Technology for Metallic Materials, South China University of Technology, Guangzhou 510640, People's Republic of China. Contact e-mail: yzhliu@scut.edu.cn
Manuscript submitted December 30, 2011.
Article published online June 30, 2012

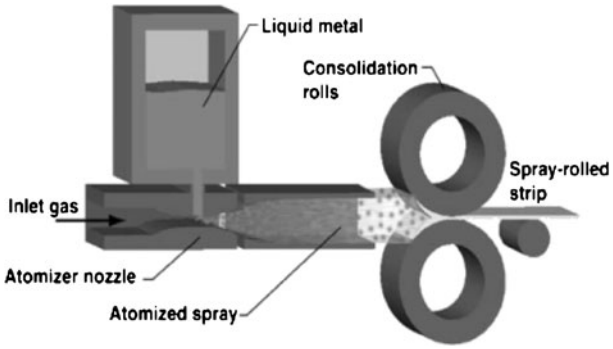

Fig. 1—Schematic of spray rolling.[1]

$$m(r,h) = m_{\max 0} \cdot \left(\frac{h_0}{h}\right)^2 \exp\left(-a_0 \cdot \left(\frac{h_0}{h}\right)^k r^k\right) \quad [1]$$

where k is a constant, r presents the width of the spray cone, and a_0 is a radial distribution coefficient. Once the maximum mass flux in the spray cone $m_{\max 0}$ ($\mathrm{kgm^{-2}s^{-1}}$) at a reference spray distance h_0 is known, the distribution of mass flux $m(r, h)$ at any other position can be calculated. For deposition onto the surface of a rotating mandrel with a radius R at a rotational speed ω, the coordinate transformation of an arbitrary point (r, h) can be expressed as: $r = x + \delta/2 + R$; $h = H + R - y$, where H is the spray distance and δ is the distance between two rollers.

B. *Sticking Efficiency*

When gas-atomized droplets impinge the substrate or the deposit, a part of droplets was splashed or rebounded away from the deposition surface. Usually, sticking efficiency SE is defined to express the sticking ability of the impinging droplets. This coefficient depends on several factors: the residual liquid fraction and kinetic energy of the impinging droplets, the impact angle, the thermal conditions of the deposition surface, and the interaction between the deposition surface and the droplets. For deposition onto the surface of a rotating mandrel where the geometrical effect is a dominant factor for droplet deposition, the sticking efficiency in spray rolling should relate to the droplet impact angle at deposition. Mathur *et al.*[16] proposed the sticking efficiency SE which included both thermal sticking efficiency $SE(T)$ and geometrical sticking efficiency $SE(\theta)$.

$$SE = SE(T) + SE(\theta) \quad [2]$$

where T is the temperature and θ is the impact angle between the incident mass and the surface normal at the point of deposition, *e.g.*, θ_1 in Figure 2(b). For simplicity, a mean sticking efficiency $SE(T) = 0.76$ was selected to avoid the coupling of the thermal analysis with the shape model.[17,18] Based on consideration of the geometrical effect of a rotating mandrel on droplet deposition, a geometrical sticking efficiency $SE(\theta) = 0.76 \times \cos\theta$ was assumed for 7050 aluminum alloy.[16]

C. *Deposition, Redeposition, and the Deposit Growth in Thickness*

As shown in Figure 2(b), when gas-atomized droplets impinge the substrate, a fraction of the arriving mass is retained on the surface at the point of impact, and it contributes to the growth of the surface. The primary deposition mass flux m_1 at a point (r, h) is given by

$$m_1 = g \cdot SE \cdot m(r,h) \quad [3]$$

where g is a coefficient defined as a visibility index. The considered substrate surface faces to the spray directly; thus, g is set to 1. Rebounding is found to be important for large solid droplets. The scattered mass flux from the deposition point is m_s. Mass conservation gives

$$m_s = (1 - SE) \cdot m_i(r,h) \quad [4]$$

The scattered mass either redeposits on the surface or is lost as overspray. As shown in Figure 2(b), the scattering mass flux m_{2s} was assumed to be distributed with the scattering angle θ_2 and governed by a mass scattering function $B(\theta_i)$. The total redeposition mass flux m_2 over the entire deposition surface ds is given by

$$m_2 = \frac{1}{ds} \cdot \int_{\Omega} (1 - SE) \cdot m(r,h) \cdot B(\theta_i) \cdot d\Omega \quad [5]$$

where Ω denotes the deposition surface.

The deposition of individual droplets, initially on the surface of rollers and subsequently on the previously deposited material's surface, is a sequence of discrete events. The formation of deposit shape occurs by successive accumulation of discrete droplets. The deposit growth in thickness ΔT_{thick} is given by

$$\Delta T_{\text{thick}} = (g \cdot SE \cdot m_1 + m_2) \cdot \frac{1}{\rho} \cdot \Delta t \quad [6]$$

where ρ is the density of deposited materials.

D. *Numerical Algorithm*

We can calculate the deposit shape by the method of "curve tracking." As shown in Figure 2(a), a tangent line from the atomizer to the roller determines the limiting positions for deposition onto the roller surface. The tangent point A(x_0, y_0) corresponds to the starting angle θ_0 of the spray deposition

$$\theta_0 = \pi - \arctan\left(\frac{H+R}{(\delta/2+R)^{0.5}}\right) - \arccos\left(\frac{R}{\left((R+\delta/2)^2+(H+R)^2\right)^{0.5}}\right) \quad [7]$$

Once spray rolling is initiated, the position changes from point A to point C in time Δt, as shown in Figure 3(a). This can be divided into two processes that

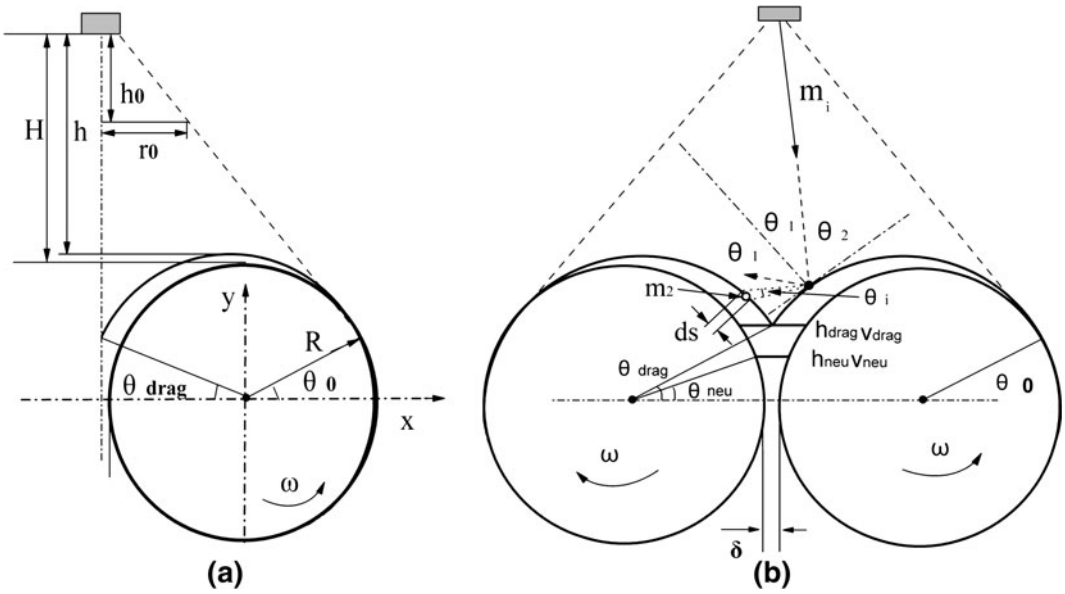

Fig. 2—(*a*) Relative geometrical position of the spray cone to the roller wheel. (*b*) A schematic illustration of droplet scattering and redeposition.

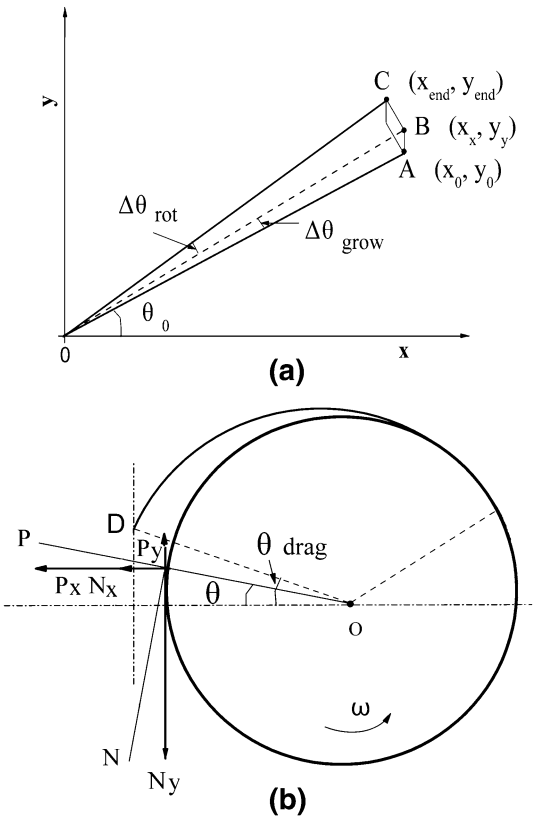

Fig. 3—(*a*) A method of "curve tracking." (*b*) Schematic diagram for the rejecting force and drag-in force.

occur simultaneously. The position moves from A(x_0, y_0) to B(x_x, y_y) due to thickening of the deposited materials with arrival of the atomized droplets at roller surface, where $y_y = y_0 + \Delta T_{\text{thick}}$ and $x_x = x_0$, the angle $\Delta\theta_{\text{grow}}$ in every time moment Δt is given by: $\Delta\theta_{\text{grow}} = \arctan(y_y/x_x) - \arctan(y_0/x_0)$. Then, the position B($x_x$, y_y) moves to C(x_{end}, y_{end}) due to rotation of the roller surface, the angle $\Delta\theta_{\text{rot}}$ in every time moment Δt is given by: $\Delta\theta_{\text{rot}} = \omega\Delta t$. Therefore, the coordinates of point C (x_{end}, y_{end}) is given by

$$\begin{aligned} y_{\text{end}} &= (y_0 + \Delta T_{\text{thick}})\sin(\theta_0 + \Delta\theta_{\text{grow}} + \Delta\theta_{\text{rot}})/ \\ &\quad r\sin(\theta_0 + \Delta\theta_{\text{grow}}) \\ x_{\text{end}} &= x_0\cos(\theta_0 + \Delta\theta_{\text{grow}} + \Delta\theta_{\text{rot}})/ \\ &\quad \cos(\theta_0 + \Delta\theta_{\text{grow}}) \end{aligned} \qquad [8]$$

At each computational time step, the rotational angle variation $\Delta\theta$ in time Δt is equal to the sum of $\Delta\theta_{\text{grow}}$ and $\Delta\theta_{\text{rot}}$. The mass fluxes associated with droplet primary deposition and redeposition are given by Eqs. [3] and [4], the growth of each surface patch over a time step is determined through a numerically integrating Eq. [6]. Then the coordinates of the deposition surface during spray rolling are obtained, updated and tracked over all the computational time steps.

E. *Determination of Drag-In Angle*

As a result of thickening, the material deposited on the two roller surfaces overlaps eventually at point D(x_{drag}, y_{drag}), as shown in Figure 3(b). The drag-in angle θ_{drag} is determined as

$$\theta_{\text{drag}} = arctan\left(y_{\text{drag}}/\left(R^2 - y_{\text{drag}}^2\right)^{0.5}\right) \qquad [9]$$

As shown in Figure 3(b), the overlapping of the deposited material at point D means the beginning of a steady state (the geometry of the deposited materials on the roller surface maintaining its top surface profile) during the spray-rolling process. When the vertical component of the radial rolling force N_y ($\theta_{\text{drag}}N\cos\theta$, where N is the radial rolling force) is larger than the

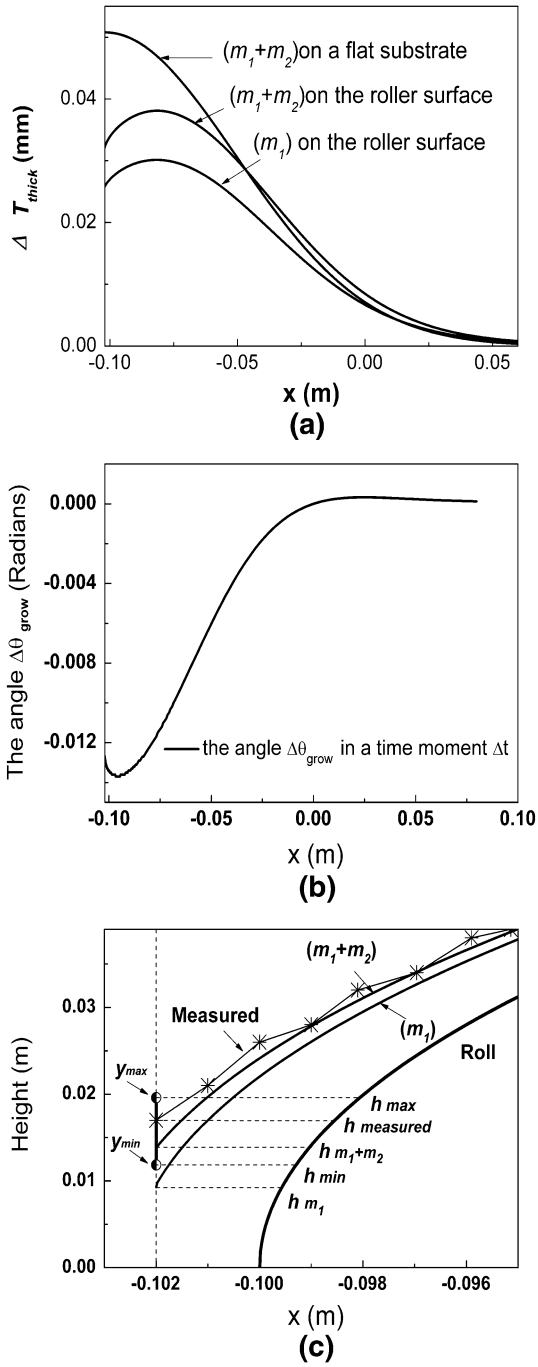

Fig. 4—Spatial distribution of ΔT_{thick} at a spray distance of 0.4 m (*a*) and the angle $\Delta\theta_{grow}$ (*b*) in a time moment Δt on a roller surface. (*c*) Comparison of simulated and experimental results of the deposit cross-sectional final shape.

vertical component of the friction force P_y ($P\sin\theta$), the metal can be dragged into the rollers successfully. In other words, the drag-in angle should not exceed the maximum value θ_{max}, where $\theta_{max} = \tan^{-1}\mu$. 7050 aluminum alloy is chosen as the material model in this work. The friction coefficient μ between the roller and Al alloy is 0.2.[19] Thus, the maximum drag-in angle (θ_{max}) is 0.1972 radians.

F. *Determination of Production Rate*

Under steady-state conditions, as shown in Figure 2(b), the mass conservation during the spray-rolling process can be described by[20]

$$M = \rho_{drag} h_{drag} v_{drag} = \rho_{neu} h_{neu} v_{neu} \quad [10]$$

where M is the production rate (kgs^{-1} per meter of nozzle length) and v (ms^{-1}) is the velocity of the rolled materials along the rolling direction. h_{neu} *and* h_{drag} are the thickness of the spray-rolled materials at the rolling neutral plane and entry plane, respectively. The value of h_{neu} is given by $h_{neu} = D - D \times \cos\theta_{neu} + \delta$, where θ_{neu} is the neutral angle. The value of v_{neu} is equal to that of the rollers, $v_{neu} = R \times \omega \times \cos\theta_{neu}$. In the case of the spray-rolling process, Bland's methodology is still valid[4,21]; *i.e.*, the radial rolling pressure at the side from the rolling entry plane to the neutral plane is equal to that at the side from the neutral plane to the rolling exit plane, which leads to the following equation for the neutral angle:

$$\theta_{neu} = \sqrt{\frac{\delta}{R}}\tan\left[\frac{1}{2}\tan^{-1}\left(\sqrt{\frac{R}{\delta}}\theta_{drag}\right) - \frac{1}{2\mu}\ln\left(\frac{h_{drag}}{\delta}\right)\sqrt{\frac{\delta}{R}}\right] \quad [11]$$

If the drag-in angle and the thickness of the spray-rolled material in the entry plane are known, then the strip production rate can be calculated.

III. RESULT AND DISCUSSION

A. *Droplet Scattering and Redeposition*

For deposition of 7050 aluminum alloy on two tool steel mandrels with a diameter of 0.2 m, a fixed roll gap of 0.004 m, rolling at 3.14 rps and a spray distance of 0.4 m, the calculated ΔT_{thick} in a time moment Δt conforms to different Gaussian distributions, as shown in Figure 4(a). In this case, the value of m_{max0} is determined as 50 $kgm^{-2}s^{-1}$ at a referenced spray distance of 0.4 m. The distribution of ΔT_{thick} on a rotating mandrel expands a lower peak at the center of the deposition region compared with that on a flat substrate. By comparing the primary deposition only (m_1) with the primary deposition plus redeposition ($m_1 + m_2$), the droplet redeposition contributes 16 pct to the ΔT_{thick} by calculation. It is evident that the geometrical features of the deposition surface and the droplet redeposition of materials are important factors in governing the deposit shape. The contribution of $\Delta\theta_{grow}$ on $\Delta\theta$ at different deposition positions is demonstrated in Figure 4(b). When the value of x is greater than 0, $\Delta\theta_{grow}$ means positive, if not, $\Delta\theta_{grow}$ means negative. However, the effect of $\Delta\theta_{grow}$ on $\Delta\theta$ is small compared with that of $\Delta\theta_{rot}$.

The cross-sectional final shapes of a deposit under a steady state obtained by experiments and simulation are shown in Figure 4(c). It can be seen that the calculated cross-sectional final shape of a deposit using the

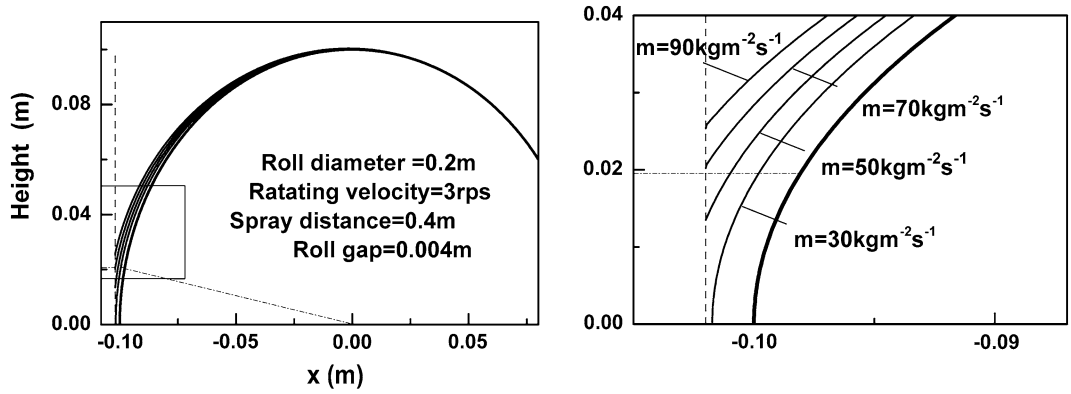

Fig. 5—Effect of maximum mass flux in the spray cone on the deposit thickness.

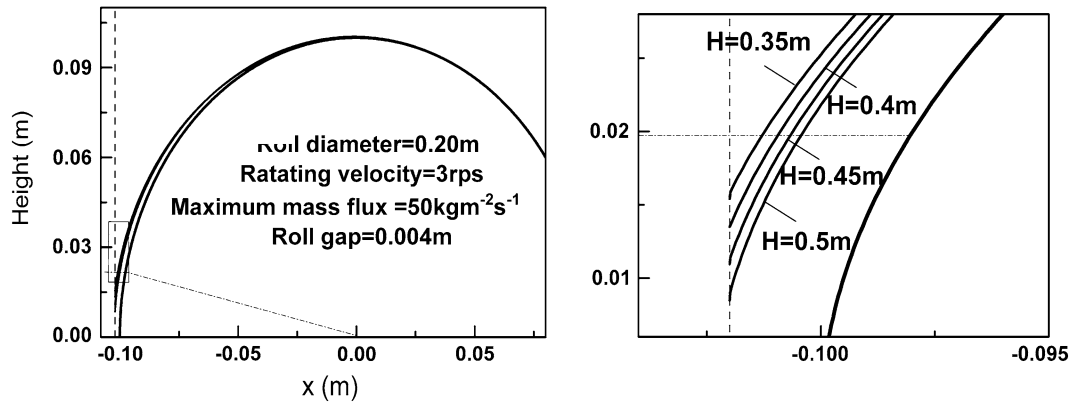

Fig. 6—Effect of spray distance on the deposit thickness.

deposition plus redeposition model agrees well with that by experiments. Compared with the calculated value of h_{m1} 0.0049 m taking no account of any redeposition, the calculated value of h_{m1+m2} taking account of redeposition is 0.0059 m, which matches closely the measured value of $h_{measured}$ 0.0065 m by experiments. Also, the calculated value of h_{m1+m2} consists well within the range of h_{min} 0.0054 to h_{max} 0.0079 m (*i.e.*, the range of y_{min} 0.01184 to y_{max} 0.01959) obtained by McHugh *et al.* under the same conditions in Reference 4. The deviation between the simulated and experimental contours at the center of the deposition region is due to the experimental limitations. In the spray-rolling process, spray cannot be stopped simultaneously. The substrate receives additional deposits, and thus, the deposit thickness increases in the experiment.

Moreover, the experimental results can be used to verify the analytic model by strip production rate. Compared with the calculated value of M 3.64 kgs^{-1}per meter of nozzle length taking no account of any redeposition, the calculated value of M considering redeposition is 3.69 kgs^{-1} per meter of nozzle length, which agrees with the measured value of M 3.72 kgs^{-1} per meter of nozzle length by experiments. The calculated values agree with the experimental data very well. At present, the production rates reported during the spray-rolling process can reach approximately 2.5 to15 kgs^{-1} per meter of nozzle length.[4,22]

B. *Influence of Processing Parameters on Deposit Shape Evolution*

The method described above was applied in a series of examples to demonstrate the effect of the processing parameters on deposit shape evolution under a steady state. According to the experimental conditions, the typical ranges of processing parameters considered in the simulation are as follows: maximum mass flux in the spray cone m_{max0} ranges from 30 to 90 $kgm^{-2}s^{-1}$, gap between the two mill rollers δ ranges from 0.002 to 0.005 m, roller diameters D ranges from 0.2 to 0.35 m, rotational frequency of rollers ω ranges from 2.5 to 4 rps, and spray distance H ranges from 0.35 to 0.5 m. The rotational angle varies from θ_0 to π. From Figure 5 to Figure 9, it is found that the deposit thickness and size increase gradually with rotational angle.

The maximum mass flux in the spray cone has a significant influence on the deposit thickness, as shown in Figure 5. The deposited material with a maximum mass flux of $30kgm^{-2}s^{-1}$ cannot be observed to overlap and contact each other. When the maximum mass fluxes in the spray cone are 50 and 90 $kgm^{-2}s^{-1}$, the values of the drag-in angle at which the materials deposit on the surface of two rollers overlap to contact each other are 0.1354 radians and 0.2563 radians, respectively. Obviously, the deposit thickness with a large mass flux is relatively thick compared with that with a small melt maximum mass flux. However, in the case of 90 $kgm^{-2}s^{-1}$ maximum mass flux,

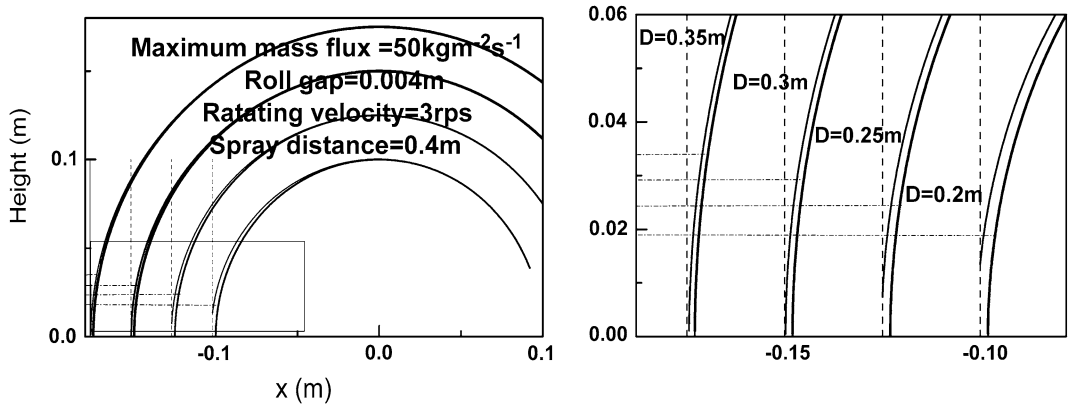

Fig. 7—Effect of roller diameter on the deposit thickness.

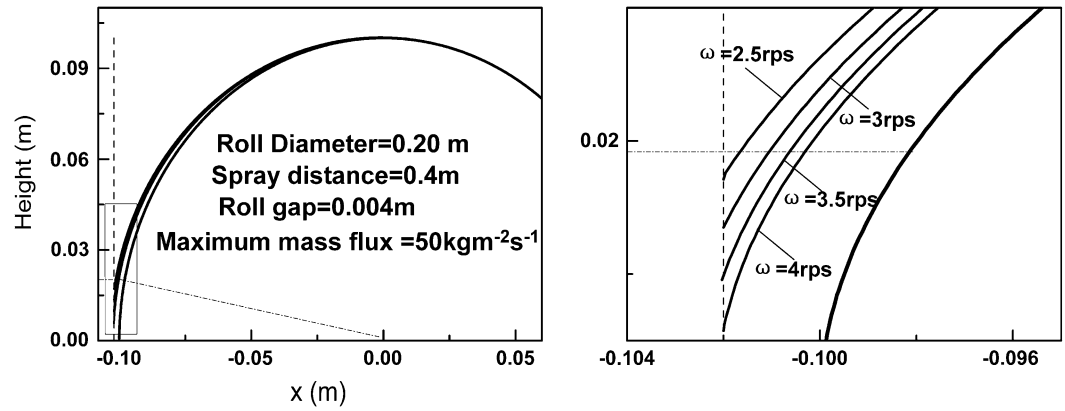

Fig. 8—Effect of roller rotational speed on the deposit thickness.

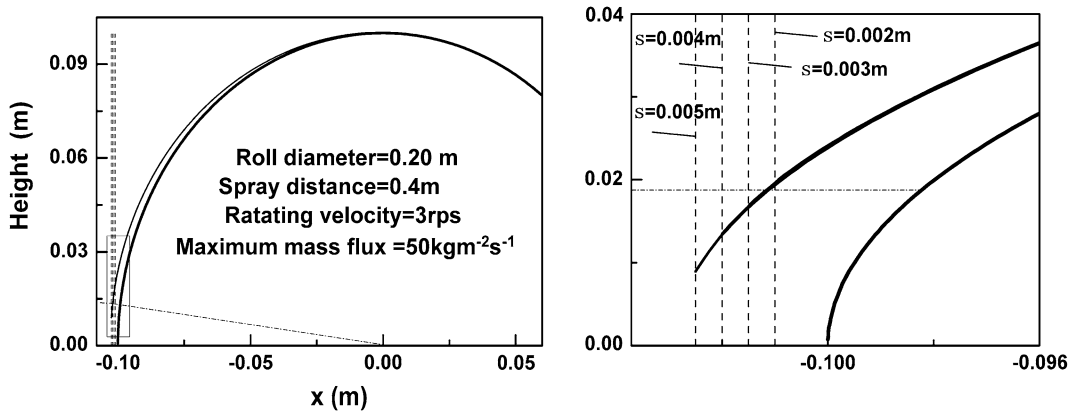

Fig. 9—Effect of roll gap on the deposit thickness.

the deposited materials can be observed to overlap and contact each other but cannot be pulled into the gap of two rollers because the drag-in angle does not exceed the maximum drag-in angle θ_{max} of 0.1972 radians. The maximum mass flux in the spray cone should be selected in the range of 50 $kgm^{-2}s^{-1}$ to 70 $kgm^{-2}s^{-1}$. The production rate for a maximum mass flux of 70 $kgm^{-2}s^{-1}$ increases to 3.08 kgs^{-1}per meter of nozzle length compared with 2.98 kgs^{-1} per meter of nozzle length for a maximum mass flux of 50 $kgm^{-2}s^{-1}$.

Figure 6 shows the effect of spray distance on the deposit thickness when other processing parameters are kept constant. By changing the spray distance from 0.35 to 0.5 m, the variation of deposit shape and dimension is obvious. Results suggest that the deposit thickness decreases with increasing spray distance. This is attributed to the fact that the mass flux distribution for a short spray distance is very concentrated, and most droplets hit the surface of rollers directly and only a small portion sprays off the surfaces of rollers. With

Table I. The Uniform Designs L_{16}^{*} (5^4) and the Orthogonal Table of Maximum Thickness

	m	H	R	δ	ω
Average value 1	6.268	1.801	1.258	13.411	13.133
Average value 2	0.162	0.472	25.223	1.797	0.738
Average value 3	13.117	18.935	6.415	6.633	19.947
Average value 4	14.950	13.291	1.603	12.657	0.680
Reference	14.788	18.643	23.965	11.613	19.267
F ratio	1.000	1.755	2.795	0.653	1.994
Significant			※		

increasing spray distance, excessive droplets cannot reach the substrate surface, thus the thickness is reduced. The deposited material with a spray distance of 0.35 m can be dragged into the gap between two rollers. The production rate is 3.07 kgs^{-1} per meter of nozzle length.

The deposit thickness profiles for different roller diameters are illustrated in Figure 7. The larger the roller diameter, the thinner the deposit thickness. The small diameter of a mandrel can cause a large amount of droplet overspray, which can make the deposited material thinner. However, the linear speed of a small-diameter roller surface is much slower than that of a larger one, which can make the deposited material thicker. In other words, the effect of roller rotational speed on deposit thickness is greater than that of deposition area. The roller diameter should be selected in the range of 0.2 to 0.25 m. The production rate for a roller diameter of 0.25 m increases to 4.47 kgs^{-1} per meter of nozzle length compared with 3.05 kgs^{-1} per meter of nozzle length for a roller diameter of 0.2 m.

The influence of the rotational speed of the mandrel on the deposit thickness is shown in Figure 8. A lower deposit thickness is obtained at a higher rotational speed. This is attributed to different deposition times. Moreover, the rotational speed should be selected in the range of 2.5 to 3 rps.

The thickness profiles of the deposit for different roll gaps are illustrated in Figure 9. The larger the roll gap, the thinner the deposit. This must be due to the main deposition area of the rollers with a large roll gap deviating from the center of the spray cone compared with that with a small roll gap. Thus, the deposit thickness decreases. The roll gap in this case should be in the range of 0.004 to 0.005 m. However, the production rate for a roll gap of 0.005 m increases to 3.67 kgs^{-1} per meter of nozzle length compared with 3.05 kgs^{-1} per meter of nozzle length for a roll gap of 0.004 m.

Moreover, the determination of the minimum deposit thickness should also consider the removing of porosity and prior droplet boundaries in the deposited material.

C. *Optimization of Processing Parameters*

It is possible to optimize processing parameters quickly, easily and accurately by using an orthogonal design method. An appropriate simulation program and table are designed and arranged, with the simulation results shown in Table I. The preform geometry is sensitive to processing parameters. The diameter of roller D plays a significant role on the deposit thickness as compared with that by other processing parameters. Moreover, the effects of spray distance H and the rotational speed of the roller ω on deposit thickness are remarkable compared with that of the roll gap δ.

IV. CONCLUSIONS

During the spray-rolling process, the geometrical effect of the rotating mandrel is an important factor for droplet deposition. Both the deposition mass and redeposition mass are retained on the surface at the point of impact, and contribute to the growth of the surface at that point, which leads to a desired deposit thickness. This analytic model can be used directly to predict the corresponding drag-in angle, deposit thickness, and strip production rate, which agree well with the experimental results. In general, the rolling angle decreases with decreasing mass flux, and increasing roller diameter and rotational speed, spray distance, and roll gap. The production rate increases with increasing mass flux, roller diameter and rotational speed, spray distance, and roll gap. In this work, a method is presented to ensure a continued operation with a high production rate.

ACKNOWLEDGMENTS

The authors gratefully acknowledge the financial support of National Natural Science Foundation of China (Project No. 50774035) and the Fundamental Research Funds for the Central Universities (Grant No. 2011ZZ0010).

NOMENCLATURE

m_{max0}	maximum mass flux in the spray core ($kgm^{-2}s^{-1}$)
h_0	reference spray distance (m)
r	width of the spray cone (m)
k	a constant
R	roller radius (m)
D	roller diameter(m)
ω	rotational speed (rps)
H	spray distance (m)
δ	roll gap (m)
SE	sticking efficiency
SE(T)	thermal sticking efficiency
SE(θ)	geometrical sticking efficiency
T	temperature (K)
θ	impact angle (radian)
m_1	deposition mass flux ($kgm^{-2}s^{-1}$)
m_s	scattered mass flux ($kgm^{-2}s^{-1}$)
m_{2s}	redeposition mass flux ($kgm^{-2}s^{-1}$)
m_2	total redeposition mass flux ($kgm^{-2}s^{-1}$)
g	visibility coefficient
B (θ_i)	mass scattering function

θ_1	mass deposition angle (radian)
θ_2	mass scattering angle (radian)
Ω	deposition surface
ΔT_{thick}	deposit growth in thickness (m)
ρ	density (kgm^{-3})
t	time (s)
θ_0	starting angel (radian)
$\Delta\theta_{\text{grow}}$	angle changed due to thickening of the deposited materials (radian)
$\Delta\theta_{\text{rot}}$	angle changed due to rotation of the roller surface (radian)
θ_{drag}	drag-in angle (radian)
N	radial rolling force (N)
P	friction force (N)
θ_{max}	maximum drag-in angle (radian)
μ	friction coefficient
M	production rate (kgs^{-1} per meter of nozzle length)
v	velocity of the rolled materials (ms^{-1})
h_{neu}	thickness of the rolled material at the neutral plane (m)
h_{drag}	thickness of the rolled material at the entry plane (m)
θ_{neu}	neutral angle (radian)

REFERENCES

1. K.M. McHugh, J.P. Delplanque, S.B. Johnson, E.J. Lavernia, Y. Zhou, and Y. Lin: *Mater. Sci. Eng. A*, 2004, vol. 383A, pp. 96–106.
2. A.R.E. Singer: *Metall. Trans.*, 1970, vol. 4, pp. 246–57.
3. K.M. McHugh, Y. Lin, Y. Zhou, S.B. Johnson, J.P. Delplanque, and E.J. Lavernia: *Mater. Sci. Eng. A*, 2008, vol. 477A, pp. 26–34.
4. Y.J. Lin, K.M. McHugh, Y. Zhou, and E.J. Lavernia: *Metall. Mater. Trans. A*, 2004, vol. 35A, pp. 3595–3603.
5. Y.J. Lin, K.M. McHugh, Y. Zhou, and E.J. Lavernia: *Metall. Mater. Trans. A*, 2004, vol. 35A, pp. 3633–39.
6. S.B. Johnson, J.P. Delplanque, and Y. Lin: *Proc. 2nd Int. Conf. on Spray Deposition and Melt Atomization and the 5th Int. Conf. on Spray Forming*, Bremen, Germany, 2003.
7. K.M. McHugh, E.J. Lavernia, Y. Zhou, Y.J. Lin, J.P. Delplanque, and S.B. Johnson: *Hot Deformation of Aluminum Alloys III*, Z. Jin, A. Beaudoin, T. Bieler, and B. Radhakrishnan, eds., TMS, Warrendale, PA, 2003, pp. 443–52.
8. J.P. Delplanque, S.B. Johnson, E.J. Lavernia, Y. Zhou, Y. Lin, and K.M. McHugh: *Hot Deformation of Aluminum Alloys III*, Z. Jin, A. Beaudoin, T. Bieler, and B. Radhakrishnan, eds., TMS, Warrendale, PA, 2003, pp. 433–41.
9. C. Cui, U. Fritsching, and A. Schulz: *Metall. Mater. Trans. A*, 2007, vol. 38A, pp. 333–46.
10. M.P. Kanouff, R.A. Neiser, and T.J. Roemer: *J. Therm. Spray. Tech.*, 1998, vol. 7, pp. 219–28.
11. Z. Djuri′c, P. Newbery, and P. Grant: *Model. Simul. Mater. Sci. Eng.*, 1999, vol. 7, pp. 553–71.
12. S. Markus, C. Cui, and U. Fritsching: *Mater. Sci. Eng. A*, 2004, vol. 38A, pp. 166–74.
13. J. Mi and P.S. Grant: *Acta Mater.*, 2008, vol. 56, pp. 1588–96.
14. N.H. Pryds, J.H. Hattel, T.B. Pedersen, and J. Thorborg: *Acta Mater.*, 2002, vol. 50, pp. 4075–91.
15. C. Cui, U. Fritsching, A. Schulz, and Q. Li: *Acta Mater.*, 2005, vol. 53, pp. 2765–74.
16. P. Mathur, S. Annavarapu, D. Apelian, and A. Lawley: *Mater. Sci. Eng. A*, 1991, vol. 142A, pp. 261–76.
17. M. Buchholz, V. Uhlenwinkel, and N. Ellendt: *Proc. 4th Int. Conf. on Spray Forming*, A. Leatham, ed., Baltimore, MD, 1999, pp. 13–15.
18. M.F. Smith, R.A. Neiser, and R.C. Dykhuizen: *Proc. 7th National Spray Conference*, Boston, MA, 1994, pp. 603–08.
19. A.D. Sarkar and J. Clarke: *Wear*, 1980, vol. 61, pp. 157–67.
20. J.N. Harris: *Mechanical Working of Metals*, Pergamon Press Ltd., Oxford, U.K., 1983, pp. 112–14.
21. R. Bland and H. Ford: *Proc. Inst. Mech. Eng.*, 1948, vol. 159, p. 144.
22. K.M. McHugh: *P/M in Aerospace, Defense and Demanding Applications—1995*, F.H. Froes, ed., Metal Powder Industries Federation, Princeton, NJ, 1995, pp. 345–53.